SPE 84228

Drift-Flux Modeling of Multiphase Flow in Wellbores

H. Shi[1], SPE, J.A. Holmes[2], SPE, L.J. Durlofsky[1, 3], SPE, K. Aziz[1], SPE, L.R. Diaz[1], SPE, B. Alkaya[1], SPE, and G. Oddie[4]
[1]Stanford University, [2]Schlumberger GeoQuest, [3]ChevronTexaco EPTC, [4]Schlumberger Cambridge Research

This paper was prepared for presentation at the SPE Annual Technical Conference and Exhibition held in Denver, Colorado, U.S.A., 5 – 8 October 2003.

Abstract

Drift-flux modeling techniques are commonly used to represent two and three-phase flow in pipes and wellbores. Unlike mechanistic models, drift-flux models are continuous, differentiable and relatively fast to compute, so they are well suited for use in wellbore flow models within reservoir simulators. Drift-flux models require a number of empirical parameters. Most of the parameters used in current simulators were determined from experiments in small diameter (2 inch or less) pipes. These parameters may not be directly applicable to flow in wellbores or surface facilities, however, as the flow mechanisms in small pipes can differ qualitatively from those in large pipes. In order to evaluate and extend current drift-flux models, an extensive experimental program was initiated. The experiments entailed measurement of water-gas, oil-water and oil-water-gas flows in a 15 cm diameter, 11 m long plexiglass pipe at 8 deviations ranging from vertical to slightly downward. In this paper, these experimental data are used to determine drift-flux parameters for steady state two-phase flows of water-gas and oil-water in large-diameter pipes at inclinations ranging from vertical to near-horizontal. The parameters are determined using an optimization technique that minimizes the difference between experimental and model predictions for holdup. It is shown that the optimized parameters provide considerably better agreement with the experimental data than do the existing default parameters.

Introduction

Multiphase flow effects in wellbores and pipes can have a strong impact on the performance of reservoirs and surface facilities. In the case of horizontal or multilateral wells, for example, pressure losses in the well can lead to a loss of production at the toe or overproduction at the heel. In order to model and thereby optimize the performance of wells or reservoirs coupled to surface facilities, accurate multiphase pipeflow models must be incorporated into reservoir simulators.

Within the context of petroleum engineering, the three types of pipeflow models most commonly used are empirical correlations, homogeneous models and mechanistic models. Empirical correlations are based on the curve fitting of experimental data and their applicability is generally limited to the range of variables explored in the experiments. These correlations can be either specific for each flow pattern or can be flow pattern independent. Homogeneous models assume that the fluid properties can be represented by mixture properties and single-phase flow techniques can be applied to the mixture. These models can also allow slip between the phases and this requires a number of empirical parameters. Homogeneous models with slip are called drift-flux models.

Mechanistic models are in general the most accurate as they introduce models based on the detailed physics of each of the different flow patterns. From a reservoir simulation perspective, however, mechanistic models can cause difficulties because they may display discontinuities in pressure drop and holdup at some flow pattern transitions. Such discontinuities can give rise to convergence problems within the simulator. One approach to avoid these convergence issues is to introduce smoothing at transitions. An alternative approach is to apply a homogeneous pipeflow model. The drift-flux model is in fact a simple mechanistic model for intermittent flows, and it is used within general mechanistic models when the flow pattern is predicted to be bubble or slug.

Homogeneous models have the advantages of being relatively simple, continuous and differentiable. As a result, they are well suited for use in reservoir simulators. The simplest homogeneous models, which neglect slip between the fluid phases (i.e., the fluid phases all move at the same velocity), are not appropriate for use in reservoir simulators because they fail to capture the complex relationship between the in situ volume fraction and the input volume fraction. Drift-flux models, by contrast, are a good choice for use in reservoir simulators as they do account for the slip between the fluid phases. Drift-flux models are additionally capable of modeling counter-current flow, which allows the heavy and light phases to move in opposite directions when the overall flow velocity is small or when the well is shut in. For this reason, the drift-flux model is used in a number of reservoir simulators (e.g., in the multi-segment well model in the

ECLIPSE® black oil and compositional reservoir simulators[1,2]).

Drift-flux models require a number of empirical parameters. Most of the parameters used in current simulators were determined from experiments in small diameter (2 inch or less) vertical pipes. These parameters may not be directly applicable to wellbore flows, however, as the flow mechanisms in small pipes can differ qualitatively from those in large pipes (Jepson and Taylor[3]). It is therefore important that the drift-flux parameters be determined for wellbores and pipes of sizes of practical interest.

The overall goal of our work in this area is the development of optimized drift-flux models for use in reservoir simulators. In order to accomplish this, extensive experimental and modeling efforts were initiated. The experimental work, reported in detail by Oddie *et al.*[4], entailed large-diameter (6 inch) pipeflow experiments performed at a variety of phase flow rates and pipe inclinations. In our current study, these unique experimental data will be used to assess existing drift-flux models and to determine drift-flux parameters for steady state two-phase flows of water-gas and oil-water in large-diameter pipes or wellbores. The parameters are determined using an optimization technique that minimizes the difference between experimental and model predictions. It is shown that existing default parameters are suboptimal in many cases. Models to accurately represent the effect of pipe inclination are also presented.

The basic drift-flux model was first proposed by Zuber and Findlay[5]. It has since been refined by many researchers (e.g., Ishii[6], Nassos and Bankoff [7], Wallis[8], Hasan and Kabir[9-11], Ansari *et al.*[12]) and has been widely used for modeling both liquid-gas and oil-water pipeflow (Flores *et al.*[13], Petalas and Aziz[14]). The drift-flux model applies two basic parameters: the profile parameter C_0 and drift velocity V_d. Using these parameters (which in turn depend on the system variables), in situ phase volume fractions (holdup) can be calculated from the phase flow rates.

This paper proceeds as follows. We first present the detailed drift-flux model used in this work. We then provide an overview of the experimental program and describe the type and quality of the data collected. Next, we compute drift-flux model parameters from this data using an optimization technique that minimizes the difference between the experimental data and model predictions for steady state water-gas and oil-water flows. The effect of pipe inclination is also modeled.

Drift-flux Model

The drift-flux model for two-phase flow[5] describes the slip between gas and liquid as a combination of two mechanisms. One mechanism results from the non-uniform profiles of velocity and phase distribution over the pipe cross-section (see Figure 1). The gas concentration in vertical gas-liquid flow tends to be highest in the center of the pipe, where the local mixture velocity is also fastest. Thus, when integrated across the area of the pipe, the average velocity of the gas tends to be greater than that of the liquid. The other mechanism results from the tendency of gas to rise vertically through the liquid due to buoyancy.

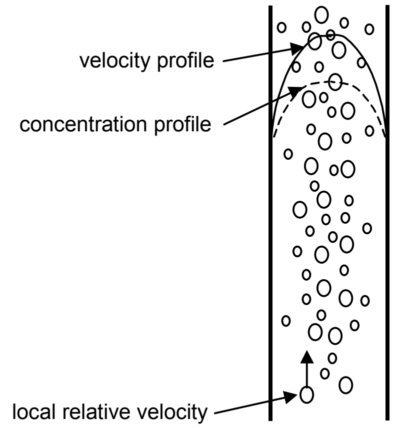

Fig. 1: Profile and local slip mechanisms in the drift-flux model

A formulation that combines the two mechanisms is[5]

$$V_g = C_0 V_m + V_d \tag{1}$$

Here V_g is the flow velocity of the gas phase, averaged across the pipe area, C_0 is the profile parameter (or distribution coefficient), which describes the effect of the velocity and concentration profiles, V_m is the volumetric flux (or average velocity) of the mixture and V_d is the drift velocity of the gas, describing the buoyancy effect.

The average mixture velocity is the sum of the gas and liquid superficial velocities,

$$V_m = V_{sg} + V_{sl} = \alpha_g V_g + (1-\alpha_g) V_l \tag{2}$$

where α_g is the in situ gas volume fraction, averaged across the area of the pipe. The average flow velocity of the liquid phase is thus

$$V_l = \frac{1-\alpha_g C_0}{1-\alpha_g} V_m - \frac{\alpha_g}{1-\alpha_g} V_d \tag{3}$$

For efficient application in a well model of a reservoir simulator, we require expressions for C_0 and V_d that are relatively simple to compute, continuous and differentiable. As will be evident below, some of the characteristics of the different flow patterns can be captured through these parameters.

The profile parameter. Zuber and Findlay[5] reported values of C_0 ranging between 1.0 and 1.5. Several drift-flux models use a value for C_0 of 1.2 in the bubble and slug flow regimes (e.g., Aziz *et al.*[15], Ansari *et al.*[12], Hasan & Kabir[9]), but in the annular mist regime the value is close to 1.0. Moreover, C_0 should approach 1.0 as α_g approaches 1.0; in fact $\alpha_g C_0$ should never exceed 1.0. Accordingly, we apply a relationship for C_0 that has a constant value at conditions equivalent to bubble or slug flow, and reduces to 1.0 as α_g approaches 1.0 or as the mixture velocity increases. A suitable expression with these properties is

® Registered trademark of Schlumberger

$$C_0 = \frac{A}{1+(A-1)\gamma^2} \quad (4)$$

The purpose of the term involving γ is to cause C_0 to reduce to 1.0 at high values of α_g or V_m. The γ parameter is given by

$$\gamma = \frac{\beta - B}{1 - B} \quad \text{subject to the limits} \quad 0 \le \gamma \le 1 \quad (5)$$

where β is a quantity that approaches 1.0 as α_g approaches 1.0, and also as the mixture velocity approaches a high value. We choose the velocity of the onset of the annular flow regime to be the velocity at which the profile slip vanishes. The transition to annular flow occurs when the gas superficial velocity V_{sg} reaches the 'flooding' value V_{sgf} that is sufficient to prevent the liquid film from falling back against the gas flow. An expression for the flooding velocity is given below in Equation (10). Accordingly, we choose the following expression for β

$$\beta = \max\left(\alpha_g \ , \ F_v \frac{\alpha_g |V_m|}{V_{sgf}}\right) \quad (6)$$

The parameters A, B and F_v can be tuned to fit the observations. A represents the value of the profile parameter in the bubble and slug flow regimes, and is defaulted to 1.2. B represents the value of the gas volume fraction, or the mixture velocity as a fraction of the flooding velocity, at which C_0 starts to drop below A. B is defaulted to 0.3. F_v is a multiplier on the flooding velocity fraction, defaulted to 1.0. Profile flattening can be made more or less sensitive to the velocity by adjusting the value of F_v.

Intuitively we would expect the gas superficial velocity $V_{sg} = \alpha_g V_g$ to increase with both α_g and V_m, so the relationship for C_0 must also satisfy

$$\frac{\partial}{\partial \alpha_g}(\alpha_g \, C_0) > 0 \quad \text{and} \quad \frac{\partial}{\partial V_m}(V_m \, C_0) > 0 \quad (7)$$

There may be problems with stability if this is not the case. Both of these criteria will be satisfied if $B < (2 - A)/A$.

The gas-liquid drift velocity. We can derive an expression for the gas-liquid drift velocity by combining data on the limits of counter-current flow made under a variety of flow conditions, and interpolating between them to avoid discontinuities. The method honors observations of gas-liquid relative velocities at low and high gas volume fractions, and joins them with a 'flooding curve' (Holmes[16]), as shown in Figure 2. The relative velocity observations relate to the rise velocity of gas through a stationary liquid. From Equations (1) and (3) we can relate this to the drift velocity,

$$V_g(V_l = 0) = \frac{V_d}{1 - \alpha_g C_0} \quad (8)$$

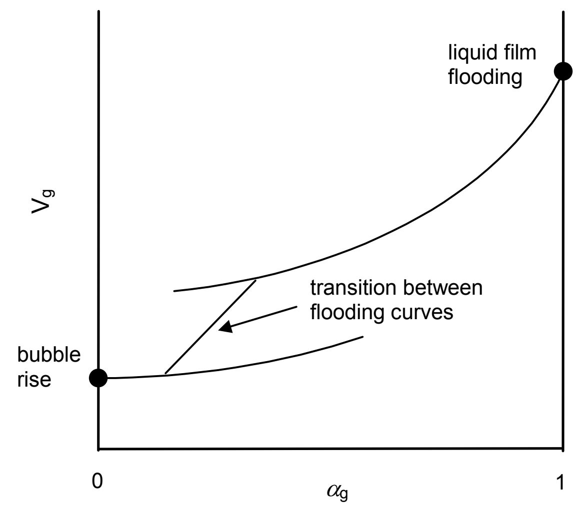

Fig. 2: Gas rise velocity in a stagnant liquid in the drift-flux model

At low values of α_g we use the rise velocity of a bubble through a stagnant liquid, which Harmathy[17] observed to be 1.53 V_c, where V_c is the characteristic velocity given by

$$V_c = \left(\frac{\sigma_{gl}\, g\, (\rho_l - \rho_g)}{\rho_l^2}\right)^{1/4} \quad (9)$$

where σ_{gl} is the gas-liquid interfacial tension.

At high values of α_g we use the 'flooding velocity', defined as the gas velocity that is just sufficient to support a thin annular film of liquid and prevent it from falling back against the gas flow. Wallis and Makkenchery[18] obtained the relation

$$V_g(V_l = 0) = K_u \left(\frac{\rho_l}{\rho_g}\right)^{1/2} V_c \quad (10)$$

where K_u is the 'critical Kutateladze number', which is related to the dimensionless pipe diameter

$$\hat{D} = \left(\frac{g(\rho_l - \rho_g)}{\sigma_{gl}}\right)^{1/2} D \quad (11)$$

according to Table 1.

Table 1. The critical Kutateladze number vs. the dimensionless pipe diameter

$\hat{D}$	K_u
≤ 2	0
4	1.0
10	2.1
14	2.5
20	2.8
28	3.0
≥ 50	3.2

To interpolate between these two extremes we make use of the flooding curve described by Wallis[8] to define the limit of the counter-current flow regime. Wallis observed that the gas and liquid flow rates that mark the limit of steady counter-current flow lie on the curve

$$\left(\frac{\rho_g}{\rho_l}\right)^{1/4}\sqrt{V_{sg}} + \sqrt{-V_{sl}} = c\left[\frac{(\rho_l-\rho_g)}{\rho_l}\,g\,D\right]^{1/4} \tag{12}$$

where c is a constant that depends on the pipe geometry. The sign convention is that upward flow is positive. We can normalize this curve to meet the flooding velocity observations in Equation (10) as $\alpha_g \to 1.0$ by substituting the right hand side of Equation (12) with $\sqrt{K_u V_c}$. Next, note that Equation (1) can be written as

$$(1-\alpha_g C_0)V_{sg} - \alpha_g C_0 V_{sl} = \alpha_g V_d \tag{13}$$

Assuming that C_0 does not vary with the flow velocity in the region of interest (the counter-current flow region), for a given value of α_g Equation (13) describes a straight line on a graph with axes V_{sg} and V_{sl}. Each of these lines should be tangential to the flooding curve – Equation (12) renormalized – which represents the limit of counter-current flow in the quadrant where $V_{sg} > 0$ and $V_{sl} < 0$. This requirement defines the drift velocity V_d as a function of α_g

$$V_d = \frac{(1-\alpha_g C_0)C_0 K_u V_c}{\alpha_g C_o\sqrt{\dfrac{\rho_g}{\rho_l}} + 1-\alpha_g C_0} \tag{14}$$

The curve must be 'ramped' down in order to match Harmathy's bubble rise velocity at low values of α_g. We apply a linear ramp between two selected values of the gas volume fraction a_1 and a_2. The overall relation for the drift velocity is thus

$$V_d = \frac{(1-\alpha_g C_0)C_0 K(\alpha_g) V_c}{\alpha_g C_o\sqrt{\dfrac{\rho_g}{\rho_l}} + 1-\alpha_g C_0} \tag{15}$$

where

$$K(\alpha_g) = 1.53/C_0 \quad \text{when } \alpha_g \le a_1$$

$$K(\alpha_g) = K_u(\hat{D}) \quad \text{when } \alpha_g \ge a_2$$

and a linear interpolation between these values when $a_1 < \alpha_g < a_2$. Setting the values of a_1 and a_2 to 0.2 and 0.4 respectively matches the data used by Zuber and Findlay[5] to demonstrate the transition from the bubble flow regime.

Oil-water slip and three-phase flow. The model described above was developed for gas-liquid flow in vertical pipes. Hasan and Kabir[11] proposed a drift-flux model for oil-water flow. The slip between oil and water is similarly described as a combination of profile and buoyancy effects

$$V_o = C_0' V_l + V_d' \tag{16}$$

For the oil-water profile parameter C_0' they suggest a value of 1.2, but this should decrease to 1.0 when oil becomes the continuous phase ($\alpha_o > 0.7$). We make C_0' a continuous function of the oil volume fraction,

$$\begin{aligned} C_0' &= A' \quad \text{when } \alpha_o \le B_1' \\ C_0' &= 1.0 \quad \text{when } \alpha_o \ge B_2' \\ C_0' &= A' - (A'-1)\left(\frac{\alpha_o - B_1'}{B_2' - B_1'}\right) \quad \text{when } B_1' < \alpha_o < B_2' \end{aligned} \tag{17}$$

The parameters A', B_1' and B_2' are adjustable and are defaulted to 1.2, 0.4 and 0.7 respectively. A condition equivalent to Equation (7) - that the oil superficial velocity should increase with the oil volume fraction - requires that $B_1' < (2-A')\,B_2'$.

For the oil-in-liquid drift velocity they suggest

$$V_d' = 1.53\,V_c'\,(1-\alpha_o)^2 \tag{18}$$

where V_c' is the characteristic velocity (Equation 9) derived with oil and water properties,

$$V_c' = \left(\frac{\sigma_{ow}\,g\,(\rho_w-\rho_o)}{\rho_w^2}\right)^{1/4} \tag{19}$$

For oil-dominated flow ($\alpha_o > 0.7$) they recommend switching to a no-slip model. But, because Equation (18) has already reduced the drift velocity by an order of magnitude when the oil volume fraction reaches 0.7, we retain that relation over the full range of α_o in order to maintain continuity.

To model three-phase (oil, water and gas) flow, we take a two-stage approach that uses the available two-phase flow models. First we combine the oil and water into a single liquid phase, with flow-weighted average properties, and determine the flow velocities of the gas and liquid phases using Equation (1). We then determine the oil and water velocities within the liquid phase using Equation (16). For this calculation we use the oil volume fraction in the liquid phase, $\alpha_{ol} = \alpha_o/(\alpha_o+\alpha_w)$. This very simplistic approach ignores any effect that the presence of a third phase may have on the respective two-phase flow models, and so must be regarded as highly tentative. Nevertheless, it does produce the expected qualitative behavior, enabling a stagnant three-phase mixture to separate into gas, oil and water zones through counter-current flow.

Inclined flow. The relationships described above are based on observations for vertical flow. Hasan and Kabir[11] proposed the following scaling for the terminal rise velocity for oil-water flow in inclined pipes

$$V_{\infty\theta} = V_\infty(\cos\theta)^{0.5}\,(1+\sin\theta)^2 \tag{20}$$

where θ is the angle of deviation from the vertical. The terminal rise velocity of a bubble or droplet is equivalent to V_d as α_o approaches zero. The rise velocity increases to about 2.5 times its value in vertical pipes, before falling off steeply to zero when the pipe is horizontal. Hasan and Kabir[11] presented their scaling as valid for oil-water flow for deviations θ < 70°. The application of Equation (20) outside these conditions and over the complete range of α can only be viewed as a tentative procedure.

Experimental setup and results

We now briefly describe the experimental setup and data that will be used for our determination of the drift-flux parameters. For a full description, see Oddie *et al.*[4]

Experimental setup. The experiments were conducted in a 10.9 m long, 15.2 cm diameter, inclinable flow-loop. The test section, shown in Figure 3, is made of plexiglass to enable visual observations. During the experiments, the pipe deviation varied from 0° (upwards vertical) to 92° (slightly downhill). Oil (kerosene with a viscosity of 1.5 cP at 18°C and a density of 810 kg/m^3) and water (tap water) were stored in a large separator and were transported separately to the inlet chamber. Another tank containing liquid nitrogen supplied gas to the pipe. This gas was first passed through evaporators and heat exchangers to allow it to reach ambient temperature. Oil, water and gas entered the pipe and flowed along the test section, where the flow pattern was observed and the pressure and holdup (as described below) were measured.

Once steady state was achieved and the steady state measurements were completed, the test section was shut in using fast closing valves. After the fluids settled, the flow-loop was rotated to the vertical if necessary so that the final positions of the fluid interfaces could be measured directly from markings on the test section. This provided the shut-in holdup. Over most of the range in holdup the error of this absolute volume measurement is less than 1%. However, volume fractions greater than 94% could not be measured accurately since the part of the test section near the outlet is manufactured from steel and so is not transparent.

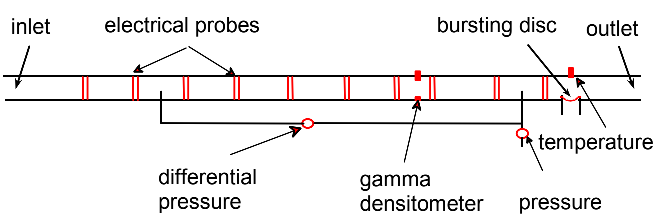

Fig. 3: Schematic of the test section of the flow loop

The other two methods used to estimate the steady state holdup were nuclear and electric probe measurements. The nuclear gamma densitometer, instrumented 7.5 m from the inlet (see Figure 3), measures the mean density of the fluid, from which the steady state holdup can be calculated. Ten electric probes were installed at various axial positions along the pipe. These probes detect the local fluid conductance, which can be used to determine the water holdup. The probes provide estimates for water holdup for both steady state and transient flows (the period following shut-in constitutes the transient stage).

The experiments were carried out over a wide range of flow rates for water, oil and gas (designated Q_w, Q_o, Q_g). For water-gas flow, $2 \le Q_w \le 100$ m^3/h and $5 \le Q_g \le 100$ m^3/h was examined, while for oil-water flow $2 \le Q_o \le 40$ m^3/h and $2 \le Q_w \le 130$ m^3/h was investigated. For three phase flows, the flow rate ranges were $2 \le Q_o \le 40$ m^3/h, $5 \le Q_w \le 40$ m^3/h, and $5 \le Q_g \le 50$ m^3/h. Different combinations of flow rates were used for the different types of tests. Note that 1 m^3/h ≈ 151 bbl/day; thus the maximum rate experiments correspond to flow rates of about 20,000 bbl/day. Each combination of flow rates was repeated at eight pipe deviations (0°, 5°, 45°, 70°, 80°, 88°, 90°, and 92° from upward vertical).

In this study, two-phase steady state data for water-gas and oil-water flows are used for the determination of drift-flux parameters. We therefore present sample data only for these two types of flows.

Steady state holdup results. As holdup is one of the most important quantities characterizing multiphase flow in wellbores, three techniques (as discussed in the previous section) were used to assess steady state holdup. We compared the three measurements in detail (see Oddie *et al.*[4]) and concluded that the resulting holdups were quite consistent overall. Since the shut-in measurement is a direct measurement, with a measurement error of less than 1% for holdup values less than 94%, we used it to represent steady state holdup. We now present a few experimental results for shut-in water holdup (referred to simply as "holdup") to provide an indication of the type and range of experimental data that will be used to determine the drift-flux model parameters.

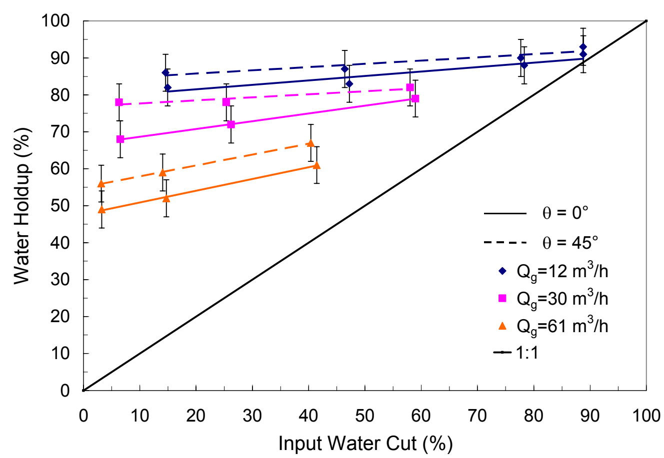

Fig. 4: Holdup for water-gas system for θ=0° and θ=45°

Figure 4 displays experimental results for water-gas systems. We present results at vertical and 45° deviation for three gas flow rates. This and subsequent plots show data in terms of water holdup versus the input water fraction or water cut (C_w). For a water-gas system, $C_w = Q_w/(Q_w + Q_g)$. The error bars indicated in the figures are ±5%, as determined from repeated experiments. The vertical distance from any point to the $\alpha_w = C_w$ line gives the slippage between the two phases. As gas flow rate increases, slippage decreases for constant input fractions. The slippage also decreases as C_w increases and as the pipe deviation shifts from 45° to vertical. As shown in Figure 5, when the pipe is further deviated from 45° to 80°, the slippage decreases. This, taken along with our measurements at 70° deviation (Oddie *et al.*[4]), indicates that the slippage displays a maximum between 45° and 70°. As we will see, the drift-flux parameters determined from the data capture this effect.

Experimental results for oil-water systems, for vertical flow and flow at 70° deviation, are presented in Figure 6. Qualitatively similar trends can be observed here as in Figures 4 and 5, though the magnitude of the effects is quite different. For example, at high flow rates (Q_o = 40 m^3/h) there is very little slippage at either inclination. At intermediate flow rates (Q_o = 10 m^3/h), by contrast, the effect of inclination is very pronounced, with much higher slippage observed at 70°. Again, our intent is to capture these complex effects via the optimized drift-flux parameters.

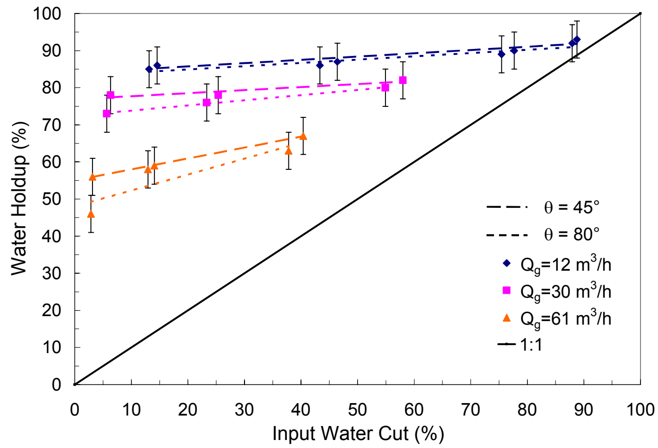

Fig. 5: Holdup for water-gas system for θ=45° and θ=80°

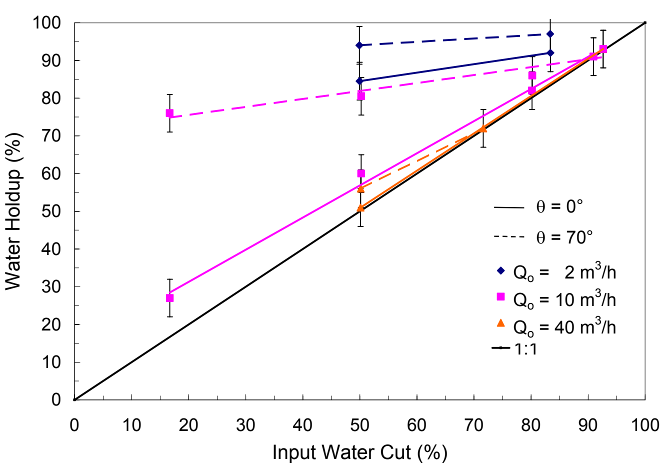

Fig. 6: Holdup for oil-water system for θ=0° and θ=70°

Parameter determination

In this section we describe the optimization procedure used to determine the drift-flux parameters. The parameters are determined such that the difference between the experimental data and model predictions for holdup are minimized in a least-square sense. We first discuss water-gas systems and then consider oil-water flows. For both systems we use experimental data for only the 6 deviations from 0° to 88° (inclusive) for the parameter determination. This is because the experimental holdup data for 90° and 92° display relatively large errors due to the way in which fluid exited the test section (Oddie *et al.*[4]).

From our earlier description of the drift-flux model, it is apparent that there are many parameters that could potentially be modified to generate close fits between the experimental and model predictions. However, we wish to avoid overly tuning the model as this may result in some parameters assuming unphysical values or in an unnecessarily complex description. We therefore performed a number of optimizations holding different sets of parameters fixed (and varying others) to determine an appropriate balance between model complexity and closeness of fit.

The parameters we ultimately chose to optimize were selected primarily based on two considerations. We optimized parameters to which the model is most sensitive as well as parameters that are the most uncertain. For example, for the water-gas system, five parameters were optimized. These include A and B, which define the shape of the C_o versus α_g curve (see Figure 7), as well as a_1 and a_2, which define the transitions in the V_d versus α_g curve (Figure 8, generated using data for a 15 cm diameter pipe). The fifth parameter optimized is a drift velocity multiplier m. This parameter is especially useful in matching data from inclined pipes, where the default relationship is given by Equation (20). Specifically, from Equation (20), the default representation for $V_{\infty\theta}$ can be written as

$$V_{\infty\theta} = V_\infty m(\theta) \tag{21}$$

where $m(\theta)$ gives the inclination effect

$$m(\theta) = (\cos\theta)^{0.5}\,(1+\sin\theta)^2 \tag{22}$$

The model is sensitive to all five of these parameters. The a_1 and a_2 transition parameters are quite uncertain as they were introduced to interpolate between models describing the two limiting cases.

The vector X_P containing the five parameters to be optimized for the water-gas system is as follows:

$$X_P = \begin{bmatrix} A & B & m & a_1 & a_2 \end{bmatrix}^T$$

The parameters are tuned to minimize the error between the experimental α_g and estimated α_g (designated α_g^*) for water-gas flows. The objective function is

$$E_{\alpha_g} = \sum_{i=1}^{N} w_i \left|\alpha_{g\,i} - \alpha_{gi}^*\right|^2 \tag{23}$$

where N is the total number of experimental data points and w_i is the weight assigned to each point, determined according to the experimental error. Experimental α_g (or α_o) less than 6% are assigned a very small value of w_i since the exact value could not be measured in this range. The minimization of E_{α_g} in Equation (23) is a nonlinear least-square problem. We apply a Levenberg-Marquardt algorithm in MATLAB[19] for this minimization.

The calculated gas holdup, computed via

$$\alpha^*_{g_i} = \frac{V_{sg_i}}{C_o(\alpha^*_g, X_P)\,V_{m_i} + V_d(\alpha^*_g, X_P)} \tag{24}$$

is obtained from the drift-flux model and the vector of parameters X_P. Because Equation (24) is implicit in $\alpha^*_{g_i}$, it must be solved using an iterative procedure. In this work a successive substitution technique is applied. The initial guess for $\alpha^*_{g_i}$ in Equation (24) is the experimental value α_{g_i}. The ranges over which the parameters in X_P may change during the optimization are specified to limit them to physically allowable values. For example, we require $1.2 \le A \le 1.5$ to maintain consistency with previous findings.

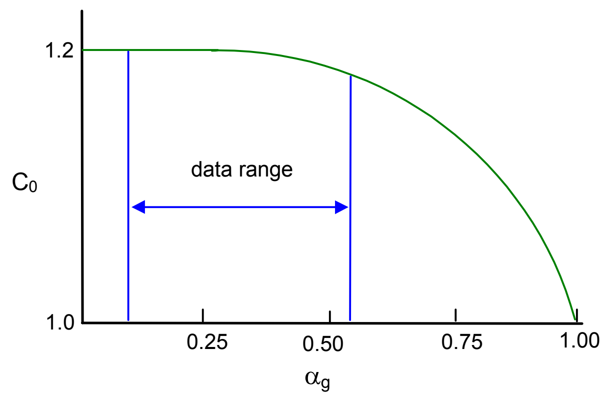

Fig. 7: Default profile parameter for water-gas system

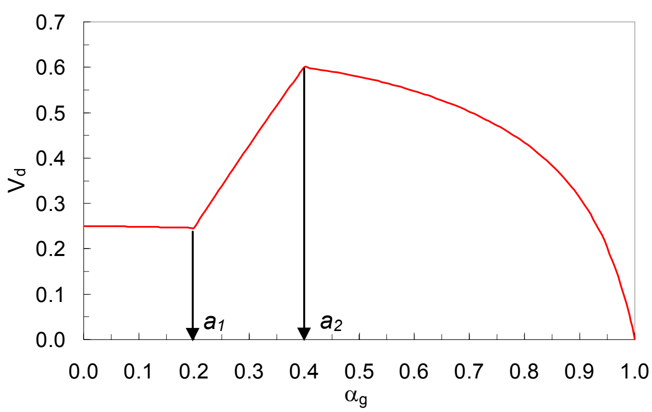

Fig. 8: Default drift velocity for water-gas system in 15.2 cm diameter pipe

For oil-water systems, we again select five parameters for optimization. Four of these parameters are analogous to those considered above: A', B_1' and B_2' (which define C_0') and the drift velocity multiplier m. We introduce an additional parameter in the expression for the oil-water drift velocity. This new parameter, designated n', replaces the exponent 2 in Equation (18). The vector of parameters to be optimized, X_P', is:

$$X_P' = \begin{bmatrix} A' & B_1' & B_2' & m & n' \end{bmatrix}^T$$

For both water-gas and oil-water flows, we first optimize the parameter values for vertical flows. We then use these values directly for deviated flows with the exception of the V_d multiplier (m), which is optimized for each deviation (i.e., as a function of θ).

Results and discussion

We now present the results for the parameter optimizations for water-gas and oil-water flows. In both cases we first determine optimized parameters for vertical flow and then consider deviated systems. We present results in terms of calculated α_g versus experimental α_g. Error is quantified as the root mean square average of the relative error of each point.

Water-gas flows. As discussed in the Introduction, the default parameters currently used in the ECLIPSE simulator were estimated, in many cases, from experiments on small-diameter (e.g., 2 inch) pipes. Thus, we would expect there to be some degree of error when these parameters are applied for large-diameter pipeflow. The predictions for α_g using these default parameters for vertical flow are shown in Figure 9. Note that we only include data for $\alpha_g > 0.06$. The level of accuracy is reasonable, though improvement is certainly possible. The root mean square error in this case is 0.297. Also shown in the figure are dashed lines designating errors of ±10% and ±20%. Four of ten points display errors of greater than 20%.

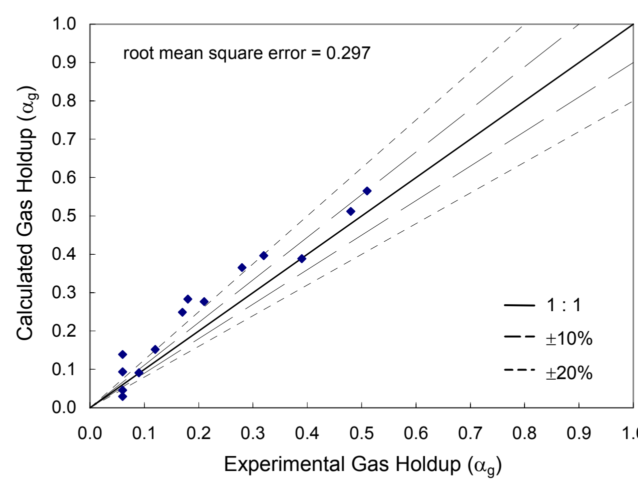

Fig. 9: Predicted gas holdup using default parameters for vertical flow (*A*=1.2, *B*=0.3, *m*=1.00, *a₁*=0.20, *a₂*=0.40)

Results for α_g using optimized parameters are shown in Figure 10. Clear improvement relative to Figure 9 is evident (root mean square error in this case is 0.070), with nearly all of the points now lying within the ±10% range. The optimized parameters used for these predictions are A=1.2, B=0.6, m =1.28, a_1 = 0.05 and a_2 =0.13. Note that this optimization gives a multiplier for V_d for the case of vertical flow (i.e., $m \neq 1$). Results of very similar accuracy, with m =1, can also be achieved using other values of the parameters. For example, using A=1.4, B=0.0, m =1.0, a_1 = 0.10 and a_2 =0.18, root mean square error was also 0.070. This illustrates that the parameter values are not unique and that there are multiple minima in the objective function. This does not appear to be a major concern, however, as the predicted α_g are in close agreement with the experimental data in either case.

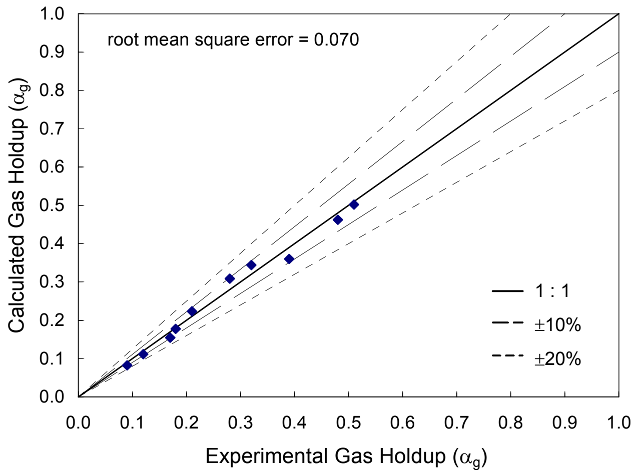

Fig. 10: Predicted gas holdup using optimized parameters for vertical flow (*A*=1.2, *B*=0.6, *m*=1.28, *a*₁=0.05, *a*₂=0.13)

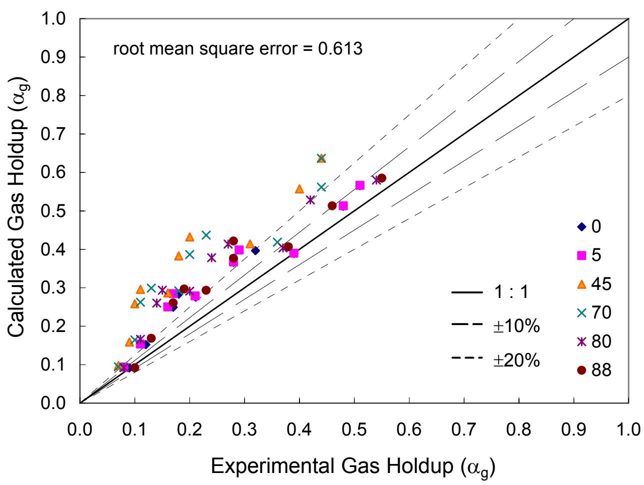

Fig. 11: Predicted gas holdup using default parameters for deviated flows (*A*=1.2, *B*=0.3, a_1=0.20, a_2=0.40)

The predictions for α_g for inclinations over the range $0 \le \theta \le 88°$, using default parameters, are shown in Figure 11. There is a clear tendency toward overprediction for $0.1 < \alpha_g < 0.3$. The error of 0.613 is quite significant for these cases. Using the optimized parameters determined for vertical flow, along with the parameter *m* optimized for each deviation, we achieve the results shown in Figure 12. The error here is reduced to only 16% of that using the defaults and all of the data now fall within the ±20% range. This improvement appears to be largely due to the reduction of a_1 and a_2 from their default values. It is worth reiterating that only V_d depends on the pipe inclination (through *m*); none of the parameters related to C_0 varies with θ.

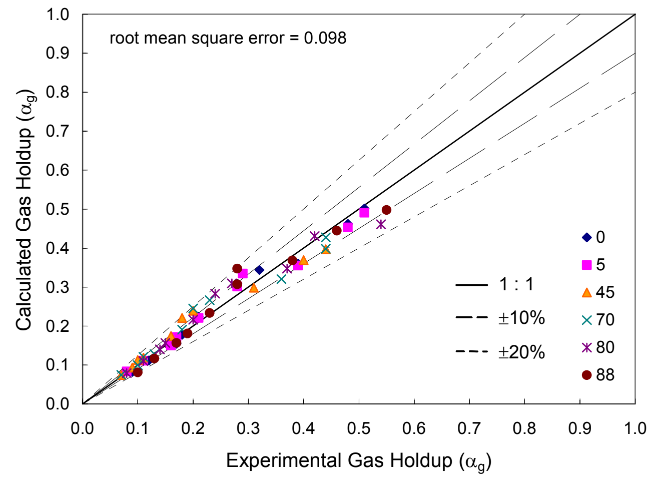

Fig. 12: Predicted gas holdup using optimized parameters for deviated flows (*A*=1.2, *B*=0.6, a_1=0.05, a_2=0.13)

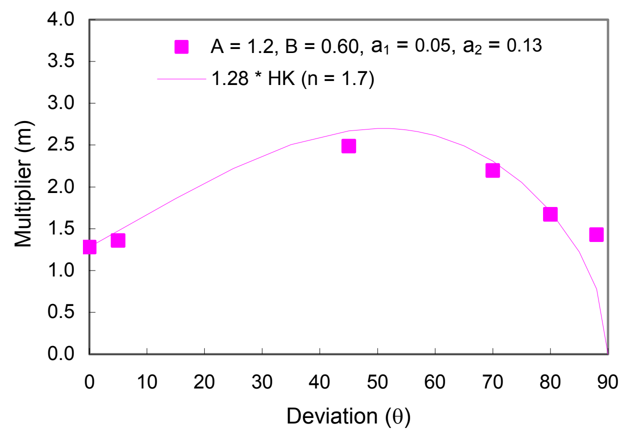

Fig. 13: Deviation effect for water-gas system

The variation of *m* (the V_d multiplier) with θ is shown in Figure 13. The values obtained from the optimization are shown as points. Note that the data do not appear to give $V_d \rightarrow 0$ as $\theta \rightarrow 90°$, suggesting that V_d is nonzero for horizontal flow. Similar observations have been made for small-diameter systems[20]. We can still attempt to fit $m(\theta)$ using the form suggested by Hasan and Kabir[11] (Equation 22). Specifically, viewing the exponent 2 as a tunable parameter *n*, we find that *n*=1.7 provides a reasonably good fit for $m(\theta)$, except for θ=88°. As indicated above, Hasan and Kabir based their model (Equation 20) on data for $\theta < 70^o$, so it is perhaps not surprising that we see deviation for larger values of θ. With the exception of this near-horizontal inclination, the following relationship provides a reasonably good fit for the drift velocity multiplier

$$m(\theta) = 1.28(\cos\theta)^{0.5}\,(1+\sin\theta)^{1.7} \qquad (25)$$

Oil-water flows. We next consider oil-water systems. The predictions for α_o using the default parameters are shown in Figure 14. The agreement here is reasonable (root mean square error of 0.159) though again some improvement is possible. Results using optimized parameters are shown in Figure 15. In this case, A'=1.0 and n'= 0.95, giving a root mean square error of 0.092. When A'=1.0, the parameters B_1' and B_2' do not enter the model since C_0' remains constant at 1.0 (see Equation 17).

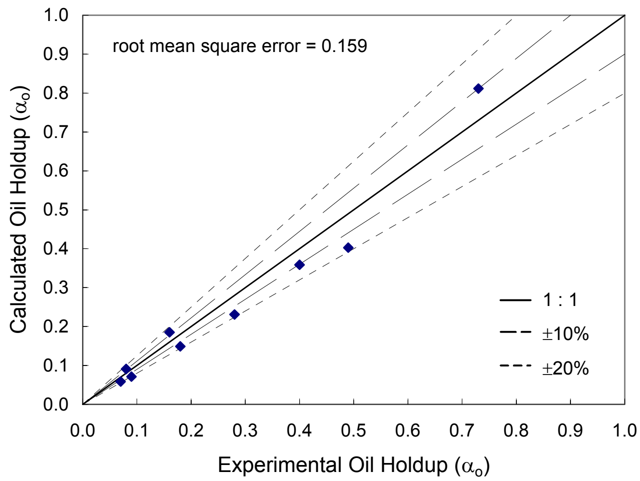

Fig. 14: Predicted oil holdup using default parameters for vertical flow (A'=1.2, B_1'=0.40, B_2'=0.70, m=1.0, n'=2.0)

Our finding that A' =1.0 (which implies that C_0' =1.0 independent of α_o) is consistent with the earlier result of Hill[21,22]. He considered oil-water flow in a 16.4 cm diameter vertical pipe (the oil was kerosene with a density of 780 kg/m^3 and a viscosity of 2 cP). Using linear regression, Hill found that C_0' =1.0. Our result is in close agreement with this observation.

The default predictions for α_o for flows in inclined pipes are presented in Figure 16. The error here is 0.555. A cluster of four points (corresponding to calculated α_o of ~0.75) is noticeably outside the 20% error line. These points all correspond to flows in which Q_o=10 m^3/h and Q_w=2 m^3/h. These flow rates are relatively low, but the input oil cut is the highest investigated. The default parameters result in significant errors for this combination of flow rates because V_d is significantly underestimated, as we will see below.

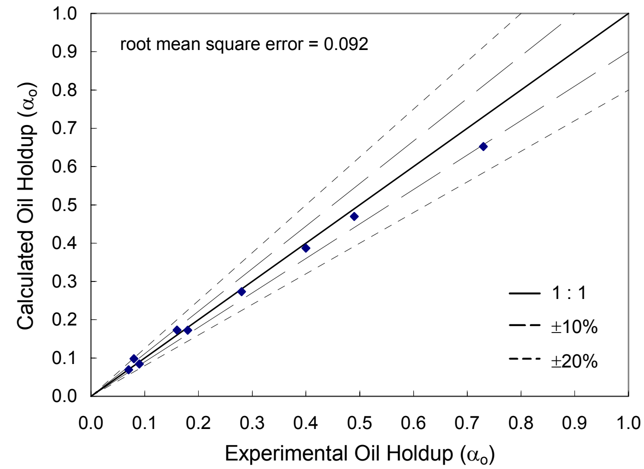

Fig. 15: Predicted oil holdup using optimized parameters for vertical flow (A'=1.0, n'=0.95)

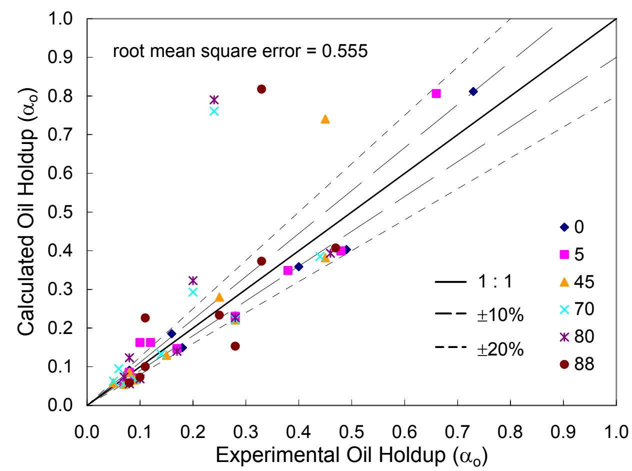

Fig. 16: Predicted oil holdup using default parameters for deviated flows (A'=1.2, B_1'=0.40, B_2'=0.70, m=1.0, n'=2.0)

Predictions using the optimized parameters are shown in Figure 17. As was the case for the water-gas systems, oil-water flow in inclined pipes is modeled using the optimized parameters for vertical flow, except for the drift velocity multiplier m which is optimized for each value of θ. Using the optimized set of parameters, the average error is reduced considerably and the four outliers now cluster around the diagonal. A few points remain outside of the ±20% range, however. The resulting variation of m with θ is shown in Figure 18. The default parameters (which provide the solid curve shown in the figure) significantly underestimate m (and thus V_d). This underestimation explains some of the error in Figure 16. The following fifth order polynomial (dashed curve) can provide the exact fit for m, but it is not recommended to apply this fit for θ > 88°:

$$m = -1.892\theta^5 + 1.488\theta^4 + 2.429\theta^3 + 0.280\theta^2 - 0.212\theta + 1.035 \quad (26)$$

where θ is in radians.

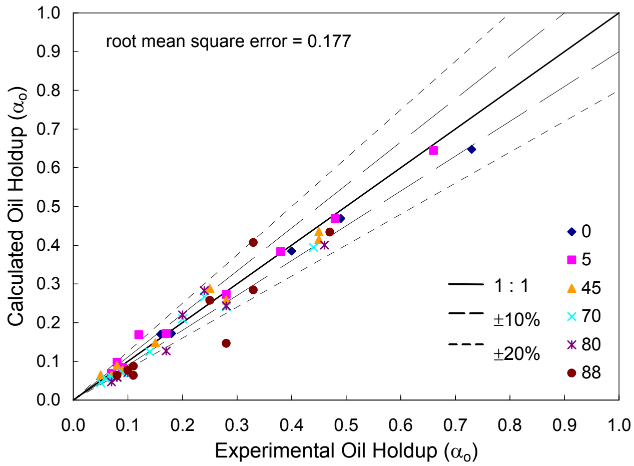

Fig. 17: Predicted oil holdup using optimized parameters for deviated flows (*A*'=1.0, *n*'=0.95)

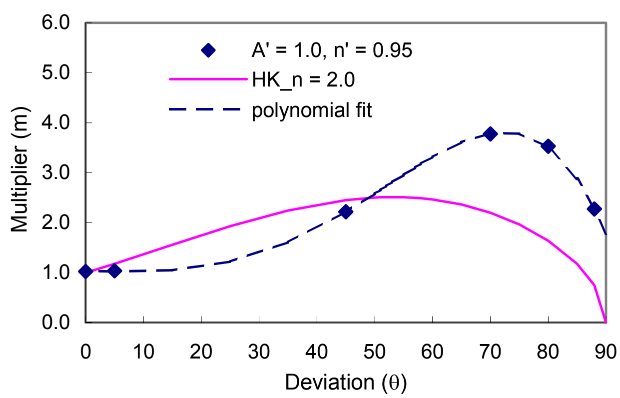

Fig. 18: Deviation effect for oil-water system

Conclusions

The drift-flux model is well suited for use in reservoir simulators because it is relatively simple and because it provides a continuous and differentiable representation of multiphase flow in pipes and wells. In this work, we used recently collected experimental data for large-diameter pipes to determine drift-flux parameters for wellbores and pipes. The following conclusions can be drawn from this study:

- Drift-flux parameters determined from experiments using small-diameter pipes (2 inch or less) may not be appropriate for use in models of flow in large-diameter wellbores.
- Drift-flux descriptions with optimized parameters can accurately describe flow in large-diameter vertical and inclined pipes for both water-gas and oil-water systems.
- Optimized parameters for flow in inclined pipes can be established by first finding optimal parameters for vertical flow and then determining a drift velocity multiplier (*m*) for each deviation.

Acknowledgments

We thank Schlumberger and the industrial affiliates of the Stanford Project on the Productivity and Injectivity of Horizontal Wells (SUPRI-HW) for their support of this work.

Nomenclature

a_1 = drift velocity ramping parameter
a_2 = drift velocity ramping parameter
A = profile parameter term, value in bubble/slug regimes for water-gas flows
A' = profile parameter term, value in bubble/slug regimes
B = profile parameter term, gas volume fraction at which C_0 begins to reduce
B_1 = profile parameter term, oil volume fraction at which C_0' begins to reduce
B_2 = profile parameter term, oil volume fraction at which C_0' falls to 1.0
C_o = profile parameter
D = pipe internal diameter
g = gravitational acceleration
K_u = Kutateladze number
m = drift velocity multiplier
n = Hasan and Kabir deviation effect parameter
n' = Hasan and Kabir drift velocity exponent
N = number of experimental points
V = velocity
V_s = superficial velocity
V_m = mixture velocity
V_d = drift velocity
V_c = characteristic velocity
X_P = vector of parameters optimized

Subscripts

g = gas
l = liquid
o = oil
w = water
m = mixture

Greek

α = holdup
β = profile parameter
γ = profile parameter reduction term
σ = interfacial tension/surface tension
ρ = density
θ = deviation from vertical

References

1. Holmes, J.A., Barkve, T. and Lund, O.: "Application of a Multisegment Well Model to Simulate Flow in Advanced Wells", SPE paper 50646 presented at the 1998 European Petroleum Conference, The Hague, October 20-22.
2. Schlumberger GeoQuest, ECLIPSE Technical Description Manual, 2001.
3. Jepson, W.P. and Taylor, R.E.: "Slug Flow and Its Transitions in Large-Diameter Horizontal Pipes", *Int. J. Multiphase Flow*, (1993) **19**, 411-420.
4. Oddie, G., Shi, H., Durlofsky, L.J., Aziz, K., Pfeffer, B. and Holmes, J.A.: "Experimental Study of Two and Three Phase

Flows in Large Diameter Inclined Pipes", *Int. J. Multiphase Flow*, (2003) **29**, 527-558.

5. Zuber, N. and Findlay, J.A.: "Average Volumetric Concentration in Two-Phase Flow Systems", *J. Heat Transfer, Trans. ASME*, (1965) **87**, 453-468.
6. Ishii M.: "One-Dimensional Drift-Flux Model and Constitutive Equations for Relative Motion Between Phases in Various Two-Phase Flow Regimes", Argonne National Lab Report, (October 1977) ANL 77-47.
7. Nassos G. P. and Bankoff S. G.: "Slip Velocity Ratios in Air-Water System Under Steady -State and Transient Conditions", *Chem. Eng. Sci. (*1967) **22**, 661-668.
8. Wallis, G.B.: *One-Dimensional Two-Phase Flow*, McGraw-Hill, 1969.
9. Hasan, A.R. and Kabir, C.S.: "A Study of Multiphase Flow Behavior in Vertical Wells", *SPE Prod. Eng*. (May 1988), 263-272.
10. Hasan A.R. and Kabir C.S.: "Predicting Multiphase Flow Behavior in a Deviated Well," *SPE Prod. Eng.* (Nov. 1988) 474-482.
11. Hasan, A.R. and Kabir, C.S.: "A Simplified Model for Oil/Water Flow in Vertical and Deviated Wellbores", *SPE Prod. & Fac*. (February 1999) 56-62.
12. Ansari, A.M., Sylvester, N.D., Sarica, C., Shoham, O. and Brill, J.P.: "A Comprehensive Mechanistic Model for Upward Two-Phase Flow in Wellbores", *SPE Prod. & Fac*. (May 1994) 143-151.
13. Flores, J.G., Sarica, C., Chen, T.X. and Brill, J.P.: "Investigation of Holdup and Pressure Drop Behavior for Oil-Water Flow in Vertical and Deviated Wells", *JERT*, *Trans. ASME* (1998) **120**, 8-14.
14. Petalas, N. and Aziz, K.: "A Mechanistic Model for Multiphase Flow in Pipes", *J. Can. Pet. Tech.* (2000) **39**, 43-55.
15. Aziz, K., Govier, G.W. and Fogarasi, M.: "Pressure Drop in Wells Producing Oil and Gas", *J. Cdn. Pet. Tech.* (July-Sep. 1972) 38-48.
16. Holmes, J.A.: "Description of the Drift Flux Model in the LOCA Code RELAP-UK", I. Mech. E. paper 206/77, Proceedings of the Conference on Heat and Fluid Flow in Water Reactor Safety, Manchester, UK, September 1977.
17. Harmathy, T.Z.: "Velocity of Large Drops and Bubbles in Media of Restricted Extent", *AIChEJ* (1960) **6,** 281.
18. Wallis, G.B. and Makkenchery, S.: "The Hanging Film Phenomenon in Vertical Annular Two-Phase Flow", *Trans. ASME*, Series I, (1974) **96**, 297.
19. The MathWorks Inc., MATLAB, 2002.
20. Franca, F. and Lahey Jr, R.T.: "The Use of Drift-Flux Techniques for the Analysis of Horizontal Two-Phase Flows", *Int. J. Multiphase Flow*, (1992) **18**, 887-901.
21. Hill, A.D.: "A Comparison of Oil-Water Slip Velocity Models Used for Production Log Interpretation", *J. Pet. Sci.& Eng.* (1992) **8**, 181-189.
22. Hill, A.D.: "Reply", *J. Pet. Sci.& Eng.* (1993) **10**, 61-65.